Chapter 5

Discussion

We have presented an overview of the theory and the measurements for both the TR method and the SCL method for dielectric and magnetic materials. In addition, relevant uncertainty analyses have been developed. Equations were presented for TR and SCL measurements that are reference plane invariant. These equations can be solved either by iteration or explicitly.

There are two common problems in the data reduction techniques for transmission line measurements. These problems are the existence of higher mode resonances and the problem that for low- loss materials the solution of the equations become ill-conditioned at integral multiples of one-half wavelength in the sample. The one-half wavelength instability occurs because the phase of S_{11} contains a large uncertainty when $|S_{11}| \rightarrow 0$ and also because the equations in this limit yield only the phase velocity. For dielectric and magnetic measurements, the uncertainty is a function of the sample length. In general for low-loss materials, samples long in relation to wavelength give more accurate results, however overmodes may be produced. Thus for broadband measurements of low-loss low-dielectric materials, it is preferable to use longer samples. However, with lossy materials, very long samples result in only front face reflection information and the results have a relatively large uncertainty. For relatively lossy materials, sample lengths on the order of one attenuation length are optimum. Longer samples allow the propagation of higher order modes, and therefore higher mode responses will be contained in measured scattering data. However, the uncertainty in the spectrum between over-moded resonance regions will be lower for longer samples than for electrically short samples.

For thicker samples the problem is more complicated and a knowledge of the uncertainty analysis is important for interpreting the results. For permeability measurements in a short-circuit line the numerical reduction procedure becomes divergent when there is an integral multiple of one-half wavelength in the sample. For TR and SCL measurements we can summarize our conclusions as follows

- For SCL measurements, length of samples should be such that $|S_{11}| \geq -20$ dB.
- The one-sample techniques appear to allow a better reduction of the scattering data.
- The optimized solution and the reference plane invariant solution appear to be the most accurate and stable methods. However, local minima have to be avoided.
- The short-circuit line is a simple way to obtain permittivity and permeability simultaneously. For low-loss materials it does suffer from numerical instabilities.
- In SCL permittivity measurements, minimum uncertainty is obtained when the sample is $\lambda/4$ from the short. This is only true for electrically thin samples.
- Minimum uncertainty magnetic measurements can be made for single frequency measurements by taking one measurement at a maximum electric field position and another measurement at a maximum magnetic field position.

The various TR and SCL techniques are compared in table 5.1 and 5.2.

Table 5.1: Dielectric and magnetic TR measurement techniques compared.

Technique	Applicability	Strong Points	Weak Points
Full 2-port, one sample	Dielectric	Requires one sample	———
Full 2-port, one sample	Magnetic	Requires one sample	Unstable at $n\lambda_m/2$
NRW Technique	Magnetic	Simple Solution	Unstable at $n\lambda_m/2$
Two-Position Technique	Magnetic	———	Doesn't exist for TR techniques
Two sample technique	Magnetic	Stable over all frequencies	Requires two samples
Multi-point techniques	Magnetic	Very stable	non-global minima

Table 5.2: Dielectric and magnetic SCL measurement techniques compared.

Technique	Applicability	Strong Points	Weak Points
One-position Technique	Dielectric	Stable	—
Two-Position Technique	Magnetic	Requires only one sample	Unstable at $n\lambda_m/2$
Two sample technique	Magnetic	Stable over all frequencies	Requires two samples
Multi-point techniques	Magnetic	Very stable	Alternative minima

We would like to thank Eleanor Livingston for her excellent comments and suggestions, Paul Domich for collaboration on the optimized solution, Chris Jones for help with measurements and plotting, William Kissick, Claude Weil, and Howard Bussey for various discussions and as sources of encouragement. Finally we would like to thank Ramon Jesch, Bill Daywitt, and Lydell Frasch for reviewing the manuscript.

References

[1] Belhadj-Tahar, N.; Fourrier-Lamer, A.; and de Chanterac, H., "Broadband simultaneous measurement of complex permittivity and permeability using a coaxial discontinuity," *IEEE Trans. Microwave Theory Tech.*, vol. 2, pp. 1–7, January 1990.

[2] Deschamps, G. A., "Determination of reflection coefficients and insertion loss of a wave-guide junction," *J. Appl. Phys.*, vol. 2, pp. 1046-1050, August 1953.

[3] "Measuring dielectric constant with the HP 8510 network analyzer," Product note no. 8510-3, Hewlett Packard, 1985.

[4] Freeman, M. S.; Nottenburg, R. N.; and DuBow, J. B., "An automated frequency domain technique for dielectric spectroscopy of materials," *J. Phys. E: Sci. Instrum.*, vol. 12, pp. 899–903, 1979.

[5] Nicolson, A. M.; and Ross, G. F., "Measurement of the intrinsic properties of materials by time domain techniques," *IEEE Trans. Instrum. Meas.*, vol. IM-19, pp. 377–382, November 1970.

[6] Weir, W. B., "Automatic measurement of complex dielectric constant and permeability at microwave frequencies," *Proc. IEEE*, vol. 62, pp. 33-36, January 1974.

[7] Stuchly, S.; and Matuszewski, M., "A combined total reflection transmission method in application to dielectric spectroscopy," *IEEE Trans. Instrum. Meas.*, vol. IM-27, pp. 285–288, September 1978.

[8] Delecki, Z. A.; and Stuchly, S. S., "Uncertainties in the determination of dielectric properties in the infinite sample method," *IEEE Trans. Instrum. Meas.*, vol. 38, pp. 902–906, June 1989.

[9] Franceschetti, G., "A complete analysis of the reflection and transmission methods for measuring the complex permeability and permittivity of materials at microwave," *Alta Frequenzia*, vol. 36, pp. 757–764, August 1967.

[10] Ligthardt, L. P., "A fast computational technique for accurate permittivity determination using transmission line methods," *IEEE Trans. Microwave Theory Tech.*, vol. MTT-31, pp. 249-254, March 1983.

[11] Roberts, S.; and von Hippel, A., "A new method for measuring dielectric constant and loss in the range of centimeter waves," *J. Appl. Phys.*, vol. 7, pp. 610–616, July 1946.

[12] Brydon, G. M.; and Hepplestone, D. J., "Microwave measurements of permittivity and $\tan\delta$ over the temperature range $20 - 700°C$," *Proc. Inst. Elec. Eng.*, vol. 112, pp. 421–425, 1965.

[13] Szendrenyi, B. B.; Kazi, K.; and Mojzes, I., "An alternative broadband method for automatic measurement of the complex permeability and permittivity of materials at microwave frequencies," *Microwave Theory and Tech. Digest*, vol. 1, no. 1, pp. 743–745, 1988.

[14] Mattar, K. E.; and Brodwin, M. E., "A variable frequency method for wide-band microwave material characterization," *IEEE Trans. Instrum. Meas.*, vol. 39, pp. 609–614, August 1990.

[15] Maze, G.; Bonnefoy, J. L.; and Kamarei, M., "Microwave measurement of the dielectric constant using a sliding short-circuited waveguide method," *Microwave J.*, pp. 77- -88, October 1990.

[16] Dakin, T. W.; and Works, C. N., "Microwave dielectric measurements," *J. Appl. Phys.*, vol. 18, pp. 789–796, September 1947.

[17] Bowie, D. M. and Kelleher, K. S., "Rapid measurement of dielectric constant and loss tangent," *IEE Trans. Microwave Theory Tech.*, vol. MTT-4, pp. 137–140, 1956.

[18] Sequeira, H. B., "Extracting μ_r and ϵ_r from one- port phasor network analyzer measurements," *IEEE Trans. Instrum. Meas.*, vol. 39, pp. 621–627, August 1990.

[19] Chao, S., "An uncertainty analysis for the measurement of microwave conductivity and dielectric constant by the short- circuited line method," *IEEE Trans. Instrum. Meas.*, vol. IM-35, pp. 36–41, March 1986.

[20] Miles, P. A., Westphal, W. P. and von Hippel, A., "Dielectric spectroscopy of ferromagnetic semiconductors," *Rev. Mod. Phys.*, vol. 29, no. 3, pp. 279–307, 1957.

[21] Solymar, L. and Walsh, D., *Lectures on Electrical Properties of Materials.* New York: Oxford University Press, 1988.

[22] Ramo, S., Whinnery, J. R. and Duzer, T. V., *Fields and Waves in Communication Electronics*. New York: John Wiley and Sons, 1984.

[23] Gilbert, T. A., "Constitutive relations," Tech. Rep., Armour Research Foundation, 1955.

[24] Hord, W. E., *Ferrite Control Components*, pp. 238–272. John Wiley and Sons, 1989.

[25] Soohoo, R. F, *Theory and Application of Ferrites*. Englewood Cliffs, NJ: Prentice-Hall, Inc., 1960.

[26] Baker-Jarvis, J., "Transmission/reflection and short-circuit line permittivity measurements," Nat. Inst. Stand. Tech. (U.S.), Tech. Note 1341, 1990.

[27] Baker-Jarvis, J., Vanzura, E. and Kissick, W. "Improved technique for determining complex permittivity with the transmission/reflection method," *IEEE Trans. Microwave Theory Tech.*, vol. 38, pp. 1096–1103, August 1990.

[28] Kerns, D. M. and Beatty, R. W., *Basic Theory of Waveguide Junctions and Introductory Microwave Network Analysis*. New York: Pergamon Press, 1967.

[29] Rasmussen, A. L., Enfield, A. W. and Hess, A. "Advances in the design and application of the radiofrequency permeameter," *Nat. Bur. Stand. (U.S.) J. Res.*, vol. 56, no. 5, pp. 261–267, 1960.

[30] Hoer, C. A. and Rasmussen, A. L., "Equations for the radiofrequency magnetic permeameter," *Nat. Bur. Stand. (U.S.) J. Res.*, vol. 67C, no. 1, pp. 69–76, 1963.

[31] Powell, R. C. and Rasmussen, A. L., "A radio-frequency permittimeter," *IRE Trans. Instrum.*, vol. I-9, no. 2, pp. 179–184, 1960.

[32] Goldfarb, R. B. and Bussey, H. E., "Method for measuring complex permeability at radio frequencies," *Rev. Sci. Instrum.*, vol. 58, no. 4, pp. 624–627, 1987.

[33] Bussey, H. E., "Measurement of rf properties of materials a survey," *Proc. IEEE*, vol. 55, pp. 1046–1053, June 1967.

[34] Westphal, W. P., "Techniques of measuring the permittivity and permeability of liquids and solids in the frequency range 3 c/s to 50 kmc/s," Laboratory for Insulation Res. Tech. Report, MIT, 1950.

[35] Bussey, H. E.; and Gray, J. E., "Measurement and standardization of dielectric samples," *IRE Trans. Instrum.*, vol. I-11, no. 3, pp. 162–165, 1962.

[36] Domich, P. A.; Baker-Jarvis J.; and Geyer, R. G., "Optimization techniques for permittivity and permeability determination," J. Res.,vol. 96, no. 5, pp. 565–575, 1991.

[37] Wallin, S. R., *Dielectric Properties of Heterogeneous Media.* PhD thesis, University of Wyoming, 1985.

[38] Papoulis, A., *Signal Analysis.* New York: McGraw-Hill, 1977.

[39] Boggs, P. T.; Donaldson, J. R; Byrd, R. H.; and Schnabel, R. B., "ALGORITHM 676 ORDPACK: software for weighted orthogonal distance regression," *ACM Trans. Math. Software*, vol. 15, no. 4, pp. 348–364, 1989.

[40] Marcuvitz, N., *Waveguide Handbook.* New York: Dover Publications, 1951.

[41] Champlin, K. S.; and Glover, G. H, "Influence of waveguide contact on measured complex permittivity of semiconductors," *J. Appl. Phys.*, vol. 37, pp. 2355–2360, May 1966.

[42] Schwinger, J. and Saxon, D. S., *Discontinuities in Waveguides.* New York: Gordon and Breach Science Publishers, 1968.

[43] Jesch, R. L., "Dielectric measurements of five different soil textural types as functions of frequency and moisture content," Nat. Bur. Stand. (U.S.) Tech. Rep., 1978.

[44] Jesch, R. L., "Dielectric measurements of oil shale as functions of temperature and frequency," *IEEE Trans. Geosci. Remote Sensing*, vol. GE-22, pp. 99–105, March 1984.

[45] Ben-Menahem, A. and Singh, S. J., *Seismic Waves and Sources.* New York: Springer-Verlag, 1981.

Chapter 7

Appendices

Appendix A

Magnetism in Matter

A.1 Description of Magnetic Phenomena

The origin of magnetism is related to the electrostatic coulomb repulsion between electrons and is intimately related to the spin and orbital angular momentum of electrons, nuclei, and other charged particles. Stern and Gerlach proved the existence of discrete magnetic moments by observing the deflection of silver atoms passing through a spatially varying magnetic field. The quantum mechanical relation between magnetic moment and angular momentum of an electron is $\vec{m}_J = -g\frac{e\hbar}{2m}\vec{J}$, where g is the Lande *g-factor* ≈ 2.002319114, $\frac{e\hbar}{2m} = 9.2742 \times 10^{-24}\ (J - m^2/W)$ is the *Bohr magneton*, $\vec{J}$ is the total quantum mechanical angular momentum, e is the electronic charge, $\hbar$ is Planck's constant, and m is the mass. The gyromagnetic ratio is defined as

$$\gamma_g = \frac{\text{magnetic dipole moment}}{\text{angular momentum}} = g\frac{e}{2m}\ . \tag{A.1}$$

There is a diversity of magnetic phenomena due to the existence of various coupling schemes of angular momenta quanta. Types of magnetism include *paramagnetism*, which is due to spin and angular momentum of individual electrons, *diamagnetism* which has its origin in the orbital angular momentum of the electron, and *ferromagnetism* originates from the formation of domains with each domain containing a large number of aligned spins.

A.1.1 Field Description of Electromagnetic Phenomena

It has been found that dielectric and magnetic phenomena are adequately described by a set of field vectors. These vectors represent the electric field, $\vec{E}$ and magnetic field, $\vec{H}$, the displacement field, $\vec{D}$, the induction field, $\vec{B}$, the polarization field, $\vec{P}$, and magnetization

field $\vec{M}$. Maxwell's equations define the spatial and temporal evolution of these field vectors. Constitutive relations between field quantities and material properties are necessary to describe electromagnetic phenomena. The displacement field is related to the electric field by $\vec{D} = \bar{\bar{\epsilon}} \cdot \vec{E}$, where $\bar{\bar{\epsilon}}$ is the permittivity tensor. For linear materials the permittivity does not depend on the field strength. The permittivity is a measure of electronic, ionic, and dipolar polarization. The permittivity is frequency dependent with dipolar polarization occurring below 10^{10} Hz, ionic polarization below 10^{13} Hz, and electronic polarization above 10^{13} Hz. The permittivity of free space is $\epsilon_0 = 8.85419\ F/m$. The magnetic field is related to the induction field by $\vec{B} = \bar{\bar{\mu}} \cdot \vec{H}$, where $\bar{\bar{\mu}}$ is the permeability tensor. The permeability of a material is a measure of the degree to which it allows the penetration by an external magnetic field. The permeability of free space is $\mu_0 = 4\pi \times 10^{-7} H/m$. The permittivity and permeability of free space are related to the speed of light in vacuum $c = 1/\sqrt{\epsilon_0 \mu_0} = 2.99792458 \times 10^8$m/sec. The electric field may contain sources, so that $\nabla \cdot \vec{E} = \rho$, where ρ is the free charge density. Induction fields are sourceless, expressed mathematically by $\nabla \cdot \vec{B} = 0$. For a charge e moving with velocity $\vec{v}$ through and electric field $\vec{E}$ and magnetic field $\vec{B}$, the Lorentz force on the charge is $F = e[\vec{E} + (\vec{v} \times \vec{B})]$.

The electronic properties of isotropic substances can be described macroscopically by scalar material properties in terms of the relative complex permittivity and permeability, ϵ_R^* and μ_R^*:

$$\epsilon = \epsilon' - j\epsilon'' = (\epsilon_R' - j\epsilon_R'')\epsilon_0 = \epsilon_R^* \epsilon_0 \ , \tag{A.2}$$

$$\mu = \mu' - j\mu'' = (\mu_R' - j\mu_R'')\mu_0 = \mu_R^* \mu_0 \ . \tag{A.3}$$

The electric and magnetic fields are modified by the presence of matter in the space-time region in and around the body. The presence of magnetism in matter is described by the magnetization vector $\vec{M}$ which quantifies the number of magnetic dipoles per unit volume. The magnetic field $\vec{H}$ is related to the induction and magnetic moment vectors by

$$\vec{H} = \frac{1}{\mu_0}\vec{B} - \vec{M} \ , \tag{A.4}$$

where μ_0 is the permeability of free space. The magnetic field is also related to the magnetization field, $\vec{M}$ by a constitutive relationship in terms of the susceptibility χ_m. For a linear medium the relation is

$$\vec{M} = \chi_m \vec{H} \ . \tag{A.5}$$

The permeability and susceptibility are related through eqs (A.4) and (A.5)

$$\mu = \mu_0(1 + \chi_m) \ . \tag{A.6}$$

Similarly, the electric field is related to the displacement field ($\vec{D}$) and the polarization field ($\vec{P}$) by

$$\vec{D} = \epsilon_0 \vec{E} + \vec{P} = \epsilon \vec{E} \ . \tag{A.7}$$

It is useful to define a constitutive relation between polarization and electric fields using the electric susceptibility (χ_{el})

$$\vec{P} = \epsilon_0 \chi_{el} \vec{E} \ , \tag{A.8}$$

and therefore

$$\epsilon = \epsilon_0 (1 + \chi_{el}) \ . \tag{A.9}$$

A.1.2 Types of Magnetism

Magnetic materials are classified by the values of permeability.

- diamagnetic $\mu' < \mu_0$,
- paramagnetic $\mu' > \mu_0$,
- ferromagnetic $\mu' >> \mu_0$.

The susceptibilities of the various classes of magnetic phenomena are

- diamagnetic $\chi_m < 0$,
- paramagnetic $\chi_m > 0$,
- ferromagnetic $\chi_m >> 0$.

Due to the complicated quantum-mechanical origin of magnetism with various competing effects, it is not always possible to classify a material into one of the categories. For example, a ferrite may be diamagnetic in X-band and paramagnetic at lower frequencies.

A.2 Paramagnetism

Paramagnetism arises from the alignment of individual spins and angular momentum of particles in external magnetic fields. Paramagnetism is an interaction between the tendency for the electron spins to be aligned with the field on the one hand and thermal agitation which tends to randomize the spins on the other hand. Paramagnetic phenomena in insulators is temperature dependent and follows Curie's law. In metals paramagnetism is strongly influenced by the conduction electrons and has minimal temperature dependence. Paramagnetic materials are primarily the rare earth and transition ions with incomplete atomic shells. There are two types of paramagnetism

- Spin paramagnetism,
- Orbital paramagnetism.

Spin paramagnetism is due to alignment of electron spins and is only slightly temperature dependent. Spin paramagnetism or Pauli paramagnetism occurs in metals. Orbital paramagnetism, caused by alignment of orbital magnetic moments, is strongly temperature dependent. This type of paramagnetism occurs in insulators.

A.2.1 Diamagnetism

Diamagnetism is the magnetic effect that is due to orbital angular momentum effects. *Larmor diamagnetism* occurs in filled-shell insulators. The origin of diamagnetism in materials is the orbital angular momentum of the electrons in applied fields. Diamagnetic materials have a negative susceptibility and generally it is not sensitive to temperature variations at least for nonsuperconducting materials. Diamagnetic materials do not have a strong magnetic response.

A.2.2 Ferromagnetism

In ferromagnetic materials, spin coupling allows regions of aligned spins to be formed, called *domains*. In each domain the spins are more or less aligned. However, adjacent domains as a whole may be arranged in a random fashion. As a magnetic field is applied the domains more or less align with the field.

The difference between paramagnetism and ferromagnetism is that in the case of the former, spins interact minimally, whereas in ferromagnetism the spins strongly interact to cause alignment. Ferromagnetic materials can exist in a nonmagnetized state since magnetic energy is at a minimum when the domains are randomly situated or in a state of maximum entropy. This random arrangement of domains is possible because it is found in a detailed analysis that it is energetically more favorable for many ferromagnetic materials to be magnetically neutral. The boundaries between the oriented spin regions, called *domain walls* require energy for formation. There is a detailed balance between the magnetic field energy caused by alignment of spins in a domain on the one hand and the energy required for domain wall formation on the other hand. Dipolar energy is decreased by wall formation, but exchange energy is increased by the Pauli exclusion principle. Domain walls are normally of 0.01 - 10 μ m thick and can deform under applied fields or mechanical stresses.

As the temperature increases in a ferromagnetic material the kinetic energy can overwhelm the magnetic energy and the preferential alignment of spins can be broken. The

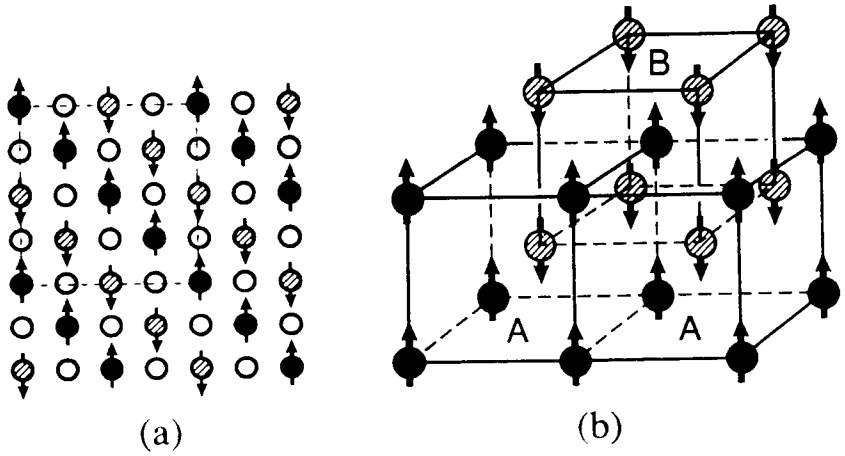

Figure A.1: Lattice structure of antiferromagnetic and ferrite materials. In one lattice the spins are up and in the other lattice the spins are down.

temperature where the kinetic thermal energy becomes predominant over the magnetic energy is called the *Curie temperature*.

If a ferromagnetic material is immersed in an increasing external field its magnetization increases. However as the external field is removed the magnetization curve does not necessarily follow the reverse curve back to the initial state; rather a slightly different curve is followed.

This phenomenon is called *hysteresis* and is caused by the irreversible movement of the domain walls. The irreversibility is caused by defects in the domain wall lattice. Thus, ferromagnetic behavior depends on the past history of the sample and is not totally reversible. Materials with large hysteresis effects are called *hard* and materials with small hysteresis effects are called *soft*.

A.2.3 Ferrites and Antiferromagnetism

Antiferromagnetism is a property possessed by many transition elements and some metals. In these materials the atoms form an ordered array with alternating spin moments so as to give zero for the net magnetic moment of the material. Antiferromagnetic materials are composed of two interpenetrating lattices. Each lattice has all spins more or less aligned, but the lattices as a whole are inverse structures as indicated in figure A.1.

Antiferromagnetic materials do not generally support permanent magnetization and do

not have a strong magnetic response to an applied field. Ferrite materials also consist of two overlapping lattices whose spins are oppositely directed, but with a larger magnetic moment in one lattice than the other. Since spin angular momentum is not canceled totally between the lattices these materials have a magnetic response to an applied field. The magnetic response increases with temperature. Antiferromagnetic materials are paramagnetic above the *Neel* temperature.

Most ferrites are mixtures of oxides such as magnetite of the generic form $XO.Fe_2O_3$ where X is a divalent metallic ion such as Fe (magnetite), Ni (nickel ferrite), Cu (copper ferrite), Mg (manganese ferrite), Co (cobalt ferrite), or Li (lithium ferrite). There are also many other spinel class ferrites that contain additional components, for example, zinc and aluminum. The spinels have either a normal or an inverse lattice structure formed by controlled quenching. Many ferrites have few free electrons and therefore are useful in microwave frequency components since the absence of free electrons prevents eddy-current losses that occur in conducting materials at high frequencies.

A.3 Equations of Motion for the Magnetization Vector

A.3.1 The Torque Equation

In this section we will develop macroscopic equations of motion that underlie the coupling of angular momentum and magnetic fields. As a model [22], we consider a spinning particle exhibiting angular momentum $\vec{J}$, immersed in a magnetic field. The presence of spin induces a magnetic moment $\vec{m} = \gamma_g \vec{J}$, where the γ_g is the gyromagnetic ratio. The magnetic field will interact with the angular momentum by inducing a torque $\vec{\tau}$

$$\vec{\tau} = \frac{d\vec{J}}{dt} . \tag{A.10}$$

We define a magnetic moment, $\vec{m} = \gamma_g \vec{J}$. The equation of motion of the spin system in an applied field $\vec{B}$ is

$$\vec{\tau} = \vec{m} \times \vec{B} , \tag{A.11}$$

or

$$\frac{d\vec{m}}{dt} = \gamma_g (\vec{m} \times \vec{B}) . \tag{A.12}$$

If we average over a significant number of these particles we obtain a macroscopic magnetic moment

$$\vec{M} = N\vec{m} \ , \tag{A.13}$$

where N = number of magnetic moments. We obtain the following equation of motion for the magnetization

$$\frac{d\vec{M}}{dt} = \gamma_g \mu (\vec{M} \times \vec{H}) + \frac{A}{\tau} \ , \tag{A.14}$$

where A is a constant and τ is a characteristic relaxation time of the system. As we will see in the next section it is possible to obtain a tensorial constitutive relation between $\vec{H}$ and $\vec{B}$ by use of eq (A.14) for a magnetic moment in an external magnetic field. This constitutive relationship will define the susceptibility and permeability tensors.

In real materials there always exists some dissipation due to damping. Dissipation is caused by such effects as magnetic dipole radiation and magneto-elastic coupling with lattice phonons. The effect of a dissipation torque can be modelled as a source term added to eq (A.14). One approximation for the dissipation torque yields the Landau equation of motion

$$\frac{d\vec{M}}{dt} = \mu\gamma_g(\vec{M} \times \vec{H}) + \underbrace{\frac{\mu\gamma_g\alpha}{|\vec{M}|}[\vec{M} \times (\vec{M} \times \vec{H})]}_{\text{damping}} \ , \tag{A.15}$$

where α is a parameter that determines the damping. This can be reduced for small damping to

$$\frac{d\vec{M}}{dt} = \mu\gamma_g(\vec{M} \times \vec{H}) + \frac{\alpha}{|\vec{M}|}[\vec{M} \times \frac{d\vec{M}}{dt}] \ . \tag{A.16}$$

This equation is due to Gilbert [23] and neglects terms nonlinear in α. The damping introduces a nonlinearity into the problem.

A.3.2 Magnetized Magnetic Material: The Polder Matrix

The constitutive relation between the induction field and the magnetic field in ferrite materials is represented by the Polder matrix. In order to derive an expression for the Polder permeability tensor we use as a model a magnetic dipole of moment $\vec{m}$, [22,24], in the presence of an external magnetic field, $H(t)$. The net torque experienced by the dipole of magnetic moment m_d is

$$\tau = -\mu m_d H(t) \sin\theta \ , \tag{A.17}$$

where θ is the angle between the dipole axis and field. In the presence of a z-axis magnetic field the dipole will precess with a characteristic Larmor frequency of $\omega_0 = |\gamma_g| H_z$ where γ_g is the gyromagnetic ratio. There are also non-conservative frictional forces present to damp the rotation.

We will assume that in the presence of a time independent d.c. magnetic field in the z direction (H_z), the magnetization is essentially at the saturated value M_s. We further assume a combined d.c. field and an alternating field $\vec{h}$, we obtain $\vec{H}(t) = H_z\vec{e}_3 + \vec{h}\exp(j\omega t)$, where $\vec{e}_3$ is the unit vector in the z direction. The magnetic moment can be approximated by $\vec{M} = M_z\vec{e}_3 + \vec{m}\exp(j\omega t)$, where M_z is time independent. When we substitute these into eq (A.16) we obtain a system of equations

$$j\omega\vec{m} = \mu\gamma_g M_s(\vec{e}_3 \times \vec{h}) + (\omega_0 + j\omega\alpha)(\vec{e}_3 \times \vec{m}) + \vec{m} \times \vec{h}\exp(j\omega t) \ , \tag{A.18}$$

where $\omega_0 = -\gamma_g H_z$ [25] and we assume $|\vec{M}| = M_s \approx M_z$. In the analysis we will neglect the last term in eq (A.18). If

$$\vec{m} = \sum_{i=1}^{3} m_i\vec{e}_i \ , \tag{A.19}$$

$$\vec{h} = \sum_{i=1}^{3} h_i\vec{e}_i \ , \tag{A.20}$$

then by substitution into eq (A.18)

$$j\omega m_x = -(\omega_0 + j\omega\alpha)m_y - \mu\gamma_g M_s h_y \ , \tag{A.21}$$

$$j\omega m_y = \gamma_g\mu M_s h_x + (\omega_0 + j\omega\alpha)m_x \ , \tag{A.22}$$

$$j\omega m_z = 0 \ . \tag{A.23}$$

Therefore

$$m_x = -\frac{(\omega_0 + j\omega\alpha)\mu\gamma_g M_s}{(\omega_0 + j\omega\alpha)^2 - \omega^2}h_x - \frac{j\omega\mu\gamma_g M_s}{(\omega_0 + j\omega\alpha)^2 - \omega^2}h_y \ , \tag{A.24}$$

$$m_y = \frac{j\omega\mu\gamma_g M_s}{(\omega_0 + j\omega\alpha)^2 - \omega^2}h_x - \frac{(\omega_0 + j\omega\alpha)\mu\gamma_g M_s}{(\omega_0 + j\omega\alpha)^2 - \omega^2}h_y \ . \tag{A.25}$$

The system of eqs (A.24) through (A.25) for the linear susceptibility relation between $\vec{M}$ and $\vec{H}$ can be expressed as

$$\mu\begin{pmatrix} \chi & -j\kappa & 0 \\ j\kappa & \chi & 0 \\ 0 & 0 & 0 \end{pmatrix}\begin{pmatrix} h_x \\ h_y \\ h_z \end{pmatrix} = \begin{pmatrix} m_x \\ m_y \\ m_z \end{pmatrix} \ , \tag{A.26}$$

where

$$\chi = \frac{(\omega_0 + j\omega\alpha)\omega_M}{(\omega_0 + j\omega\alpha)^2 - \omega^2} \ , \tag{A.27}$$

and

$$\kappa = \frac{-\omega\omega_M}{(\omega_0 + j\omega\alpha)^2 - \omega^2} , \tag{A.28}$$

and

$$\omega_M = -\gamma_g M_s . \tag{A.29}$$

We can separate out the real and imaginary components to yield

$$\chi' = \frac{\omega_M\omega_0[(\omega_0^2 - \omega^2) + \alpha^2\omega^2]}{[\omega_0^2 - \omega^2(1+\alpha^2)]^2 + 4\omega^2\omega_0^2\alpha^2} , \tag{A.30}$$

$$\chi'' = -\frac{\omega_M\omega\alpha[\omega_0^2 + \omega^2(1+\alpha^2)]}{[\omega_0^2 - \omega^2(1+\alpha^2)]^2 + 4\omega^2\omega_0^2\alpha^2} , \tag{A.31}$$

$$\kappa' = \frac{-\omega_M\omega[\omega_0^2 - \omega^2(1+\alpha^2)]}{[\omega_0^2 - \omega^2(1+\alpha^2)]^2 + 4\omega^2\omega_0^2\alpha^2} , \tag{A.32}$$

$$\kappa'' = \frac{2\omega_0\omega^2\alpha\omega_M}{[\omega_0^2 - \omega^2(1+\alpha^2)]^2 + 4\omega^2\omega_0^2\alpha^2} . \tag{A.33}$$

Note that we have assumed that the magnetization is at the saturated value M_s. That is all of the magnetic moments are assumed to be aligned with the external field. This is not always a good assumption. For this special case the Polder matrix is

$$\bar{\bar{\mu}} = \mu(\bar{\bar{I}} + \bar{\bar{\chi}}) = \mu \begin{pmatrix} \chi + 1 & -j\kappa & 0 \\ j\kappa & \chi + 1 & 0 \\ 0 & 0 & 1 \end{pmatrix} . \tag{A.34}$$

We see that in the limit as $H_z \to 0$ and $M_z \to 0$ the off-diagonal components of the permeability tensor vanish and the diagonal components reduce to the isotropic permeability, $\bar{\bar{\mu}} = \mu\ \bar{\bar{I}}$, where $\bar{\bar{I}}$ is the identity matrix.

Appendix B

Fields in Waveguides

B.1 Summary of Maxwell's Equations

Maxwell's equations are

$$\nabla \times \vec{E} = -j\omega\vec{B} \ , \tag{B.1}$$

$$\nabla \times \vec{H} = \vec{J} + j\omega\vec{D} \ , \tag{B.2}$$

$$\nabla \cdot \vec{D} = \rho \ , \tag{B.3}$$

$$\nabla \cdot \vec{B} = 0 \ . \tag{B.4}$$

The boundary conditions at material interfaces are

$$\vec{n} \times (\vec{E}_2 - \vec{E}_1) = 0 \ , \tag{B.5}$$

$$\vec{n} \times (\vec{H}_2 - \vec{H}_1) = \vec{J}_s \ , \tag{B.6}$$

$$\vec{n} \cdot (\vec{D}_2 - \vec{D}_1) = \Omega \ . \tag{B.7}$$

$$\vec{n} \cdot (\vec{B}_2 - \vec{B}_1) = 0 \ , \tag{B.8}$$

where J_s is the surface current density and Ω is the surface charge density.

B.2 Modes

B.2.1 TE Modes

The longitudinal coordinate is assumed to be z. If the H_z mode exists, it is the generator of the TE mode [22]. The TE modes satisfy the boundary value problem,

$$\{\nabla_T^2 + k_c^2\} H_{z(TE)} = 0 \ , \tag{B.9}$$

where $k_c^2 = k^2 + \gamma^2$ are real, positive eigenvalues. The boundary conditions are

$$\vec{n} \cdot (\nabla H_{(z(TE))})|_{on\ conductor} = 0 \ , \tag{B.10}$$

where $\vec{n}$ is the normal vector. Also

$$E_{z(TE)} = 0 \ . \tag{B.11}$$

The other field components are then

$$\vec{H}_{T(TE)} = -\frac{\gamma}{k_c^2} \nabla_T H_z \ , \tag{B.12}$$

$$\vec{E}_{T(TE)} = -Z_{TE}(\vec{z} \times \vec{H}_{T(TE)}) \ . \tag{B.13}$$

B.2.2 TM Modes

For the case of TM waves

$$\{\nabla_T^2 + k_c^2\} E_{z(TM)} = 0 \ , \tag{B.14}$$

where $k_c^2 = k^2 + \gamma^2$ are real, positive eigenvalues determined by boundary information on the waveguide.

The boundary conditions are

$$E_{(z(TM))}|_{on\ conductor} = 0 \ , \tag{B.15}$$

$$H_{z(TM)} = 0 \ . \tag{B.16}$$

The other field components are

$$\vec{E}_{T(TM)} = -\frac{\gamma}{k_c^2} \nabla_T E_z \ , \tag{B.17}$$

$$\vec{H}_{T(TM)} = \frac{1}{Z_{TM}}(\vec{z} \times \vec{E}_{T(TM)}) \ . \tag{B.18}$$

$$\gamma = j\sqrt{k^2 - k_c^2} \ . \tag{B.19}$$

B.2.3 TEM Modes

The propagation of *TEM* modes are possible in addition to the *TE* and *TM* modes in coaxial cable . The cutoff wave numbers for higher order *TM* waves in coaxial line are given by the roots of:

$$\frac{N_n(k_c R_1)}{J_n(k_c R_1)} - \frac{N_n(k_c R_4)}{J_n(k_c R_4)} = 0 \ , \tag{B.20}$$

[22], and for *TE* waves in coaxial line by

$$\frac{N'_n(k_c R_1)}{J'_n(k_c R_1)} \frac{N'_n(k_c R_4)}{J'_n(k_c R_4)} = 0 \ , \tag{B.21}$$

where J and N denote the Bessel functions of the first and second kind and R_1 and R_4 are the inner and outer radii respectively. The cutoff wavelengths are given approximately by:

$$\lambda_c \approx \frac{2}{q}(R_4 - R_1) \quad q = 1, 2, 3, \ldots \ . \tag{B.22}$$

For example the *TM* mode cutoff frequency in 7 mm coaxial line for eq (B.22) is approximately 34 GHz.

Appendix C

Gap Correction

C.1 Frequency-Dependent Gap Correction

C.1.1 Waveguide

We consider a sample in a rectangular waveguide of dimensions a x b with a small gap (b-d). The dielectric constant in the gap is ϵ_{Rg} and of sample ϵ_{Rs}. The measured or observed value is ϵ_{Ro}.

A transverse resonance condition yields [40]:

$$\tan(k_{1c}d) + X\tan(k_{2c}(b-d)) = 0\ , \tag{C.1}$$

where

$$k_{1c} = \frac{\omega}{c_{lab}}\sqrt{\epsilon_{Rs} - \epsilon_{Ro}}\ , \tag{C.2}$$

$$k_{2c} = \frac{\omega}{c_{lab}}\sqrt{\epsilon_{Rg} - \epsilon_{Ro}}\ , \tag{C.3}$$

and

$$X = \frac{\epsilon_{Rs}}{\epsilon_{Rg}}\frac{\sqrt{\epsilon_{Rg} - \epsilon_{Ro}}}{\sqrt{\epsilon_{Rs} - \epsilon_{Ro}}}\ . \tag{C.4}$$

For our case of waveguide $(b-d) \approx 2.54 \times 10^{-5}$ m and $b = 0.01016$ m. Equation (C.1) must be solved by iteration, but for low frequencies and low dielectric constants we can obtain a approximate solution. This equation reduces to Westphal's equation, [34] in the appropriate low frequency limit.

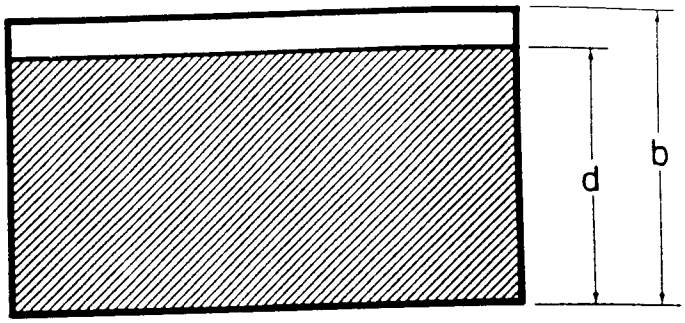

Figure C.1: Sample in waveguide with air gap.

C.1.2 Coaxial Line

For coaxial line the matching of transverse impedance yields the resonance condition [40]:

$$\mathrm{ct}(x_2, x_1) = X\,\mathrm{ct}(x_2', x_3') \ , \tag{C.5}$$

where

$$x_1 = k_{1c} R_1 \ , \tag{C.6}$$

$$x_2 = k_{1c} R_2 \ , \tag{C.7}$$

$$x_2' = k_{2c} R_1 \ , \tag{C.8}$$

$$x_3' = k_{2c} R_2 \ , \tag{C.9}$$

and X, k_{1c}, and K_{2c} are given in the previous section. The functions ct are defined as

$$\mathrm{ct}(x, y) = \frac{J_1(x)N_0(y) - N_1(y)J_0(x)}{J_0(x)N_0(y) - N_0(x)J_0(y)} \ , \tag{C.10}$$

where J_0, J_1, N_0, and N_1 are the Bessel functions of zero and first order of the first and second kind respectively.

C.2 Frequency-Independent Approaches

Various researchers have approached the gap problem by representing the sample with air gap as a layered capacitor [33,34,41]. This approach assumes that the gaps between transmission line and sample are effectively modeled by a set of capacitors in series. Champlin [41] approached the problem using as a starting point the perturbation formula developed by Schwinger [42]. By substituting into the perturbation formula approximations to the field distribution in the various regions, they obtain an estimate for the effective permittivity. Their answer turns out to be fully equivalent to the capacitor model of Westphal [34]. Champlin showed that Bussey's theory [33] is the first two terms in an expansion of Westphal [34] and Champlin's models.

The capacitor model is frequency independent and thus is strictly valid only at lower frequencies and dc. We expect the capacitor model to break down at higher frequencies because the wavelength decreases with increasing frequency to a point where multiple scattering dominates. In order to account for multiple scattering, it is necessary to develop a theory that is frequency dependent.

C.2.1 Coaxial Capacitor Model for Dielectric Materials

Consider a capacitor consisting of layers of dielectric and layers of air in a coaxial line [43,44]. The dimensions are shown in figure C.2.

We treat the system as capacitors in series, so

$$\frac{1}{C_m} = \frac{1}{C_1} + \frac{1}{C_2} + \frac{1}{C_3} \ . \tag{C.12}$$

We know that for a coaxial line the electric field distribution is given by

$$E_r = \frac{V}{\ln(\frac{b}{a})r} \ , \tag{C.13}$$

and the voltage between the conductors is given by

$$V = -\int_a^b E(r)dr \ . \tag{C.14}$$

The capacitance of a coaxial line of length L is given by

$$C = \frac{2\pi\epsilon L}{\ln\frac{R_2}{R_1}}; \tag{C.15}$$

thus, for a system of three capacitors in series we have

$$\frac{\ln\frac{R_4}{R_1}}{\epsilon'_m} = \frac{\ln\frac{R_2}{R_1}}{\epsilon'_1} + \frac{\ln\frac{R_3}{R_2}}{\epsilon'_c} + \frac{\ln\frac{R_4}{R_3}}{\epsilon'_1} \ , \tag{C.16}$$

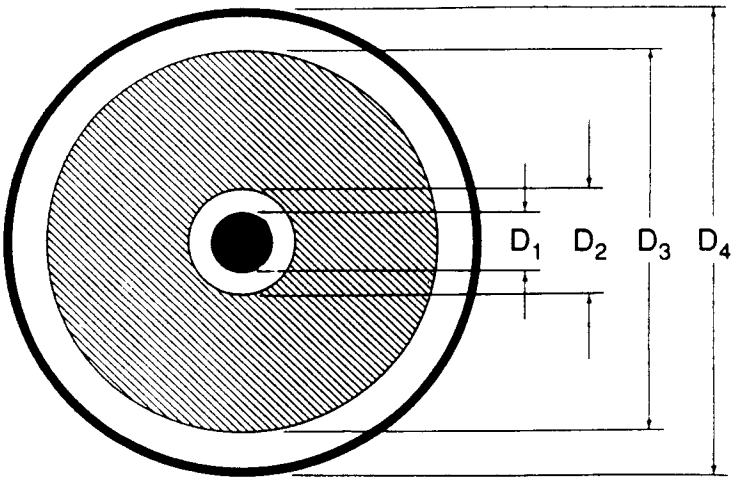

Figure C.2: A coaxial sample in holder with air gaps near conductors with diameters denoted by D_i.

where ϵ'_c, ϵ'_m are the corrected and measured values of the real part of the permittivity and ϵ'_1 is the real part of the permittivity of the air gap

$$\epsilon'_{cR} = \frac{L_2(\epsilon'_{mR}L_3 - \epsilon''^2_{mR}L_1 - \epsilon'^2_{mR}L_1)}{\epsilon'^2_{mR}L_1^2 - 2\epsilon'_{mR}L_1L_3 + \epsilon''^2_{mR}L_1^2 + L_3^2}\ , \tag{C.16}$$

$$\epsilon''_{cR} = \frac{L_2L_3\epsilon''_{mR}}{\epsilon'^2_{mR}L_1^2 - 2\epsilon'_{mR}L_1L_3 + \epsilon''^2_{mR}L_1^2 + L_3^2}\ . \tag{C.17}$$

An approximate expression is given by

$$\epsilon'_{cR} = \epsilon'_{mR}\frac{L_2}{L_3 - \epsilon'_{mR}L_1}\ , \tag{C.18}$$

$$\tan\delta_c = \tan\delta_m[1 + \epsilon'_{mR}\frac{L_1}{L_2}]\ , \tag{C.19}$$

where

$$L_1 = \ln\frac{R_2}{R_1} + \ln\frac{R_4}{R_3}\ . \tag{C.20}$$

$$L_2 = \ln\frac{R_3}{R_2}\ . \tag{C.21}$$

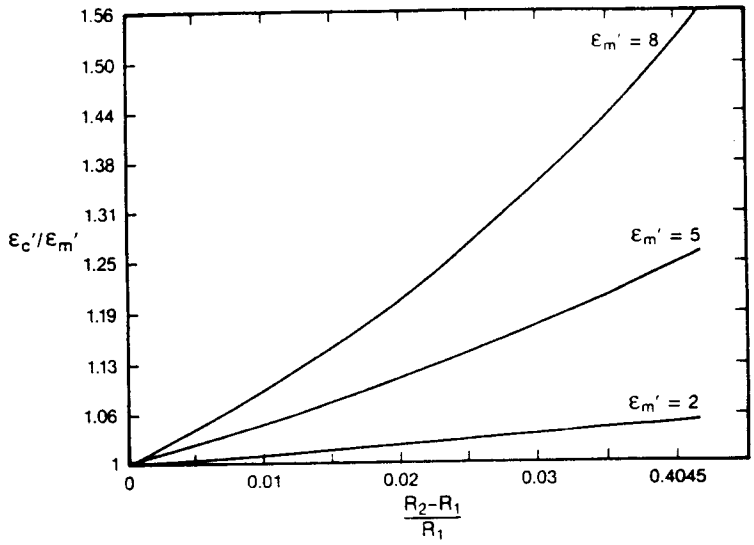

Figure C.3: The gap correction calculated for various values of ϵ'_R, where R_2, R_1 are the radii of the inner conductor and sample respectively.

$$L_3 = \ln \frac{R_4}{R_1} \,. \tag{C.22}$$

Equation (C.18) breaks down when $\epsilon'_{mR} \geq L_3/L_1$. An example is plotted in figure C.3 for a 7 mm coaxial line.

C.2.2 Rectangular Waveguide Model

For the case of a rectangular guide of short dimension b with sample thickness d and long dimension b_1 and sample thickness d_1 the E-plane gap correction is

$$\epsilon'_{cR} = \frac{d(b(\epsilon'_{mR} - \epsilon'^2_{mR} - \epsilon''_{mR}) + d(\epsilon'^2_{mR} + \epsilon''^2_{mR}))}{b^2(\epsilon'^2_{mR} - 2\epsilon'_{mR} + \epsilon''^2_{mR} + 1) - 2bd(\epsilon'^2_{mR} - \epsilon'_{mR} + \epsilon''^2_{mR}) + d^2(\epsilon'^2_{mR} + \epsilon''^2_{mR})} \,, \tag{C.23}$$

$$\epsilon''_{cR} = \frac{db\epsilon''_{mR}}{b^2(\epsilon'^2_{mR} - 2\epsilon'_{mR} + \epsilon''^2_{mR} + 1) - 2bd(\epsilon'^2_{mR} - \epsilon'_{mR} + \epsilon''^2_{mR}) + d^2(\epsilon'^2_{mR} + \epsilon''^2_{mR})} \,. \tag{C.24}$$

C.3 Gap Correction for Magnetic Materials

C.3.1 Coaxial Line

For the calculation of the gap correction for the permeability a pure inductance model is useful. We model the transmission line as

a series of inductors for the E-field gap

$$L_m = L_c + L_{air} \ , \tag{C.25}$$

where c, m, and air denote corrected value, measured value, and air space. Therefore the corrected value is

$$L_c = L_m - L_{air} \ . \tag{C.26}$$

The inductance is the flux penetrating the circuit divided by the current flowing in the circuit

$$L = \frac{\phi}{I} \ , \tag{C.27}$$

where

$$\phi = \int \vec{B} \cdot d\vec{S} \ . \tag{C.28}$$

Ampere's law is

$$\int \vec{H} \cdot d\vec{l} = I \ , \tag{C.29}$$

which yields

$$B_\phi = \frac{\mu' I}{2\pi r} \ . \tag{C.30}$$

Therefore

$$\phi = \frac{1}{2\pi} \mu' I \ln b/a \ , \tag{C.31}$$

so

$$L = \frac{1}{2\pi} \mu' \ln b/a \ . \tag{C.32}$$

Therefore we can write for the corrected permeability

$$\mu'_{cR} = \frac{\mu'_{mR} \ln R_1/R_1 - [\ln R_2/R_1 + \ln R_4/R_3]}{\ln R_3/R_2} \ , \tag{C.33}$$

$$\mu''_{cR} = \mu''_{mR} \frac{\ln(R_4/R_1)}{\ln(R_3/R_2)} \ . \tag{C.34}$$

Gap corrections are given in figures C.4- C.7. The corrections for permeability in coaxial line are much less than for permittivity. This is due to the fact the azimuthal magnetic

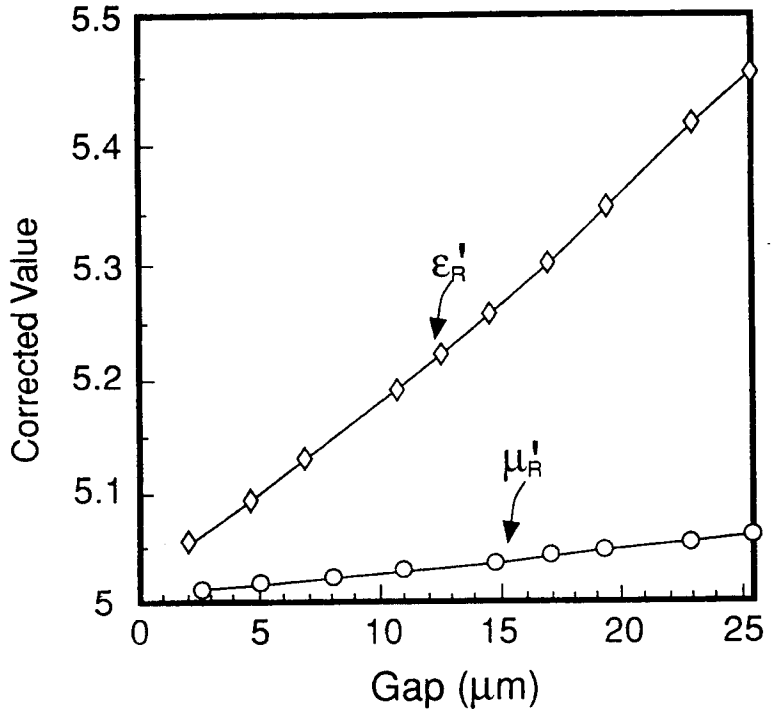

Figure C.4: Corrected permeability and permittivity as a function of inner conductor gap for a 7 mm sample. The gap around the outer conductor is assume to be zero. In this case the uncorrected (measured) was $\mu_R' = 5$, $\epsilon_R' = 5$.

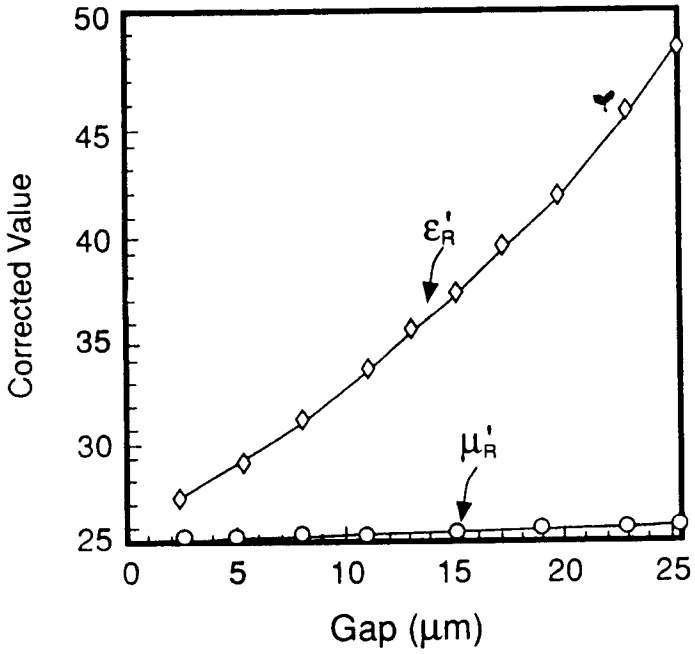

Figure C.5: Corrected permeability and permittivity as a function of inner conductor gap for a 7 mm sample. The gap around the outer conductor is assume to be zero. In this case the uncorrected (measured) was $\mu_R' = 25$, $\epsilon_R' = 25$.

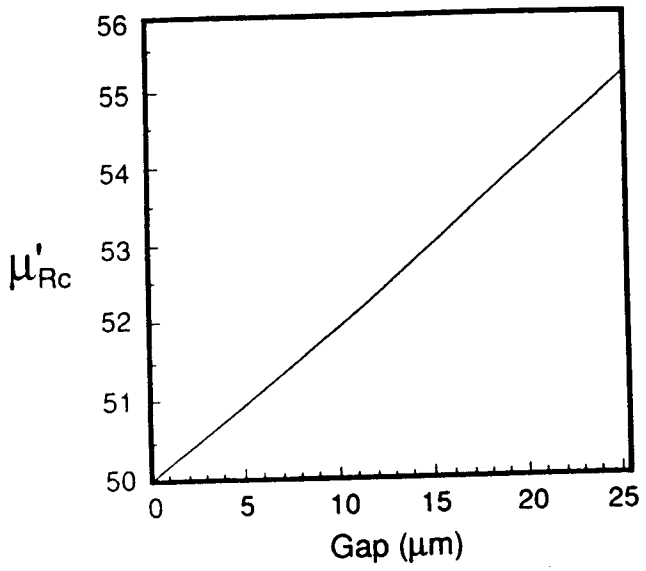

Figure C.6: Corrected permeability as a function of inner conductor gap for a 7 mm sample. The gap around the outer conductor is assume to be zero. In this case the uncorrected (measured) was $\mu'_R = 50$.

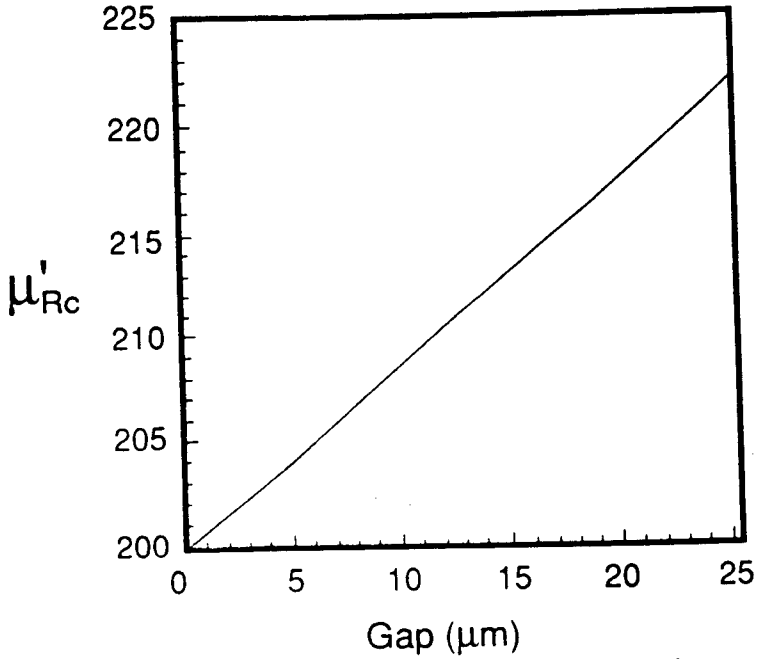

Figure C.7: Corrected permeability as a function of inner conductor gap for a 7 mm sample. The gap around the outer conductor is assume to be zero. In this case the uncorrected (measured) was $\mu'_R = 200$.

field is continuous across the discontinuity, whereas the radial electric field is discontinuous across the discontinuity.

(C.35)

C.3.2 Waveguide

E-plane Gaps

For magnetic materials in waveguide for the TE_{10} mode the E- plane gap is less severe than the H-field gap. The corrections can be obtained using inductances in series. These are

$$\mu'_{cR} = \mu'_{mR}\left(\frac{b}{d}\right) - \left(\frac{b-d}{d}\right) , \tag{C.36}$$

$$\mu''_{cR} = \mu''_{mR}\left(\frac{b}{d}\right) . \tag{C.37}$$

H-plane gaps

For the long width of the waveguide there is a discontinuity in the magnetic field for the TE_{10} mode. The corrections can be obtained using inductances in parallel. We assume a long waveguide width of b_1 and sample width d_1

$$\mu'_{cR} = \frac{d_1(b_1(\mu'_{mR} - \mu'^2_{mR} - \mu''_{mR}) + d_1(\mu'^2_{mR} + \mu''^2_{mR}))}{b_1^2(\mu'^2_{mR} - 2\mu'_{mR} + \mu''^2_{mR} + 1) - 2b_1d_1(\mu'^2_{mR} - \mu'_{mR} + \mu''^2_{mR}) + d_1^2(\mu'^2_{mR} + \mu''^2_{mR})} , \tag{C.38}$$

$$\mu''_{cR} = \frac{d_1 b_1 \mu''_{mR}}{b_1^2(\mu'^2_{mR} - 2\mu'_{mR} + \mu''^2_{mR} + 1) - 2b_1d_1(\mu'^2_{mR} - \mu'_{mR} + \mu''^2_{mR}) + d_1^2(\mu'^2_{mR} + \mu''^2_{mR})} . \tag{C.39}$$

C.4 Gap Correction Formulas Derived Directly From Maxwell's Equations

Consider Maxwell's equations in a coaxial line

$$\nabla \times \vec{E} = -j\omega\vec{B} . \tag{C.40}$$

The radial electric field is discontinuous at the air gap interface, but the displacement vector $\vec{D}$ is continuous across the interface. Also H_ϕ is continuous across the interface, whereas $\vec{B}$ is discontinuous. Let us assume that there are no sources so that $\vec{J} = 0$. Then, we can write eq (C.40) as

$$\nabla \times \frac{\vec{D}}{\epsilon} = -j\omega\mu\vec{H} \ . \tag{C.41}$$

If we now average eq (C.41) over the cross-sectional area of a coaxial line, we obtain

$$2\pi \int_a^b \nabla \times \frac{\vec{D}}{\epsilon} dr = -j\omega 2\pi \int_a^b \mu\vec{H} dr \ . \tag{C.42}$$

Continuity of the displacement field and tangential magnetic field and the fact that $D_r \propto 1/r$ and $H_\phi \propto 1/r$ is imposed and integrations are performed. Comparing these results to an effective medium equation, we obtain the same form as the previously developed capacitor and inductance models for the corrected permittivity and permeability:

$$\frac{\ln \frac{R_4}{R_1}}{\epsilon'_m} = \frac{\ln \frac{R_2}{R_1}}{\epsilon'_1} + \frac{\ln \frac{R_3}{R_2}}{\epsilon'_c} + \frac{\ln \frac{R_4}{R_3}}{\epsilon'_1} \ , \tag{C.43}$$

$$\mu'_{mR}[\ln R_4/R_1] = \mu'_{cR} \ln R_3/R_2 + [\ln R_2/R_1 + \ln R_4/R_3] \ . \tag{C.44}$$

The analogous calculation can be performed for waveguide. These effective media formulas are the Voigt approximation for the permeability (layers in series) and the Reuss approximation (layers in parallel) for the permittivity. The previously developed capacitor model can be derived directly from Maxwell's equations.

From the perspective of Maxwell's equation the limitations of the capacitor and inductance models can be assessed. In order for these models to apply, we assume that

- The fundamental mode is the only propagating mode.
- The air gap and sample are azimuthally symmetric.

The air gap modifies the modal structure in the waveguide. The model assumption that only a TEM mode is propagating in a coaxial line with an air gap around the sample becomes less and less valid as the air gap increases in size. In fact, since the phase velocity in the air gap region is much larger than the phase velocity in the sample, a distortion of the wave can be expected. Longitudinal components of the electric field and therefore TM modes will form as a result of an air gap if above cutoff. If the air gap or sample are not azimuthally symmetric, H_ϕ is no longer the only nonzero magnetic field component. This asymmetry will allow higher order TE modes to propagate, when they are above cutoff. When the assumption that the only propagating mode is the fundamental mode breaks down, equations of the same form as eqs (C.43) and (C.44) hold with the logarithmic constants replaced by more complicated expressions.

C.5 Mitigation of Air Gap Effects

It is possible to minimize the effects of air gaps by placing a conducting material in the air gap. This material may be a conducting paint, indium-gallium solder alloy, or a conducting grease. The conducting material will change the line impedance and line loss to a degree. However, for relatively small gaps, the improvements in dielectric and magnetic property measurements far outweigh any changes in line impedance. The loss measurement will be influenced by this procedure. Application of the conducting material is an art.

Appendix D

Causal Functions and Linear Response

D.1 Introduction

We call a temporal function *causal* if it is 0 for all times less than 0. The goal of this section is to review the basic mathematics used to describe causal systems.

In the analysis to follow we assume that an impulse is applied to a system at $t = 0$. We can model a linear system by an input function $f(t)$, an output function $g(t)$, and an impulse response function $a(t)$. It is possible for either or both of $f(t)$ and $a(t)$ to be causal. A more general approach would be to study nonlinear response with linear response as a very special case. Linear response theory is usually valid when the underlying probability density function can be approximated as an equilibrium distribution.

If both $f(t)$ and $a(t)$ are causal, the linear response is given by [45]

$$g(t) = \int_0^t f(\tau)a(t-\tau)d\tau \ . \tag{D.1}$$

In this case, the output is a convolution over all past times. If only $f(t)$ is causal then

$$g(t) = \int_0^\infty f(\tau)a(t-\tau)d\tau \ . \tag{D.2}$$

We assume that $a(t) = 0$ for $t < 0$. The interpretation of the function $f(t)$ can be obtained from the relationship

$$f(t) = \int_{-\infty}^\infty f(\tau)\delta(t-\tau)d\tau \ . \tag{D.3}$$

If we identify the left side of eq (D.3) as the response function, then the impulse response $a(t)$ is delta function in the special case of no distortion. Of course, in real systems the impulse response will be broader than a delta function.

We can define the step response function $h(t)$ as

$$\frac{dh(t-\tau)}{dt} = a(t-\tau) \ , \tag{D.4}$$

and it is assumed that $h(0) = 0$. If we use the step response for $g(t)$ in eq (D.1) we obtain

$$g(t) = f(0)h(t) + \int_0^t \frac{df(\tau)}{d\tau} h(t-\tau) \ . \tag{D.5}$$

D.2 Transfer Functions

If we send a signal $\exp(j\omega t)$ into a system, the response of the system is called the *transfer function* and is denoted by S. The transfer function is defined as the Fourier transform of the impulse response function

$$S(\omega) = \int_{-\infty}^{\infty} a(t) e^{j\omega t} dt \ . \tag{D.6}$$

As a consequence of the reality of $a(t)$, $S(-\omega) = S^*(\omega)$. If $F(\omega)$ is the Fourier transform of $f(t)$ we have, using the inverse Fourier transform

$$g(t) = \frac{1}{2\pi} P \int_{-\infty}^{\infty} F(\omega) S(\omega) e^{j\omega t} d\omega \ . \tag{D.7}$$

D.3 Kramers-Kronig Relations

The real and imaginary components of any causal function are related by a dispersion relation. The complex permittivity is a causal function whose real and imaginary components are related by the Hilbert transform [45]

$$\epsilon_r'(\omega) - \epsilon_{r\infty} = -\frac{2}{\pi} \int_0^{\infty} \frac{[\theta \epsilon_r''(\theta) - \omega \epsilon_r''(\omega)]}{\theta^2 - \omega^2} d\theta \ , \tag{D.8}$$

$$\epsilon_r''(\omega) = -\frac{2\omega}{\pi} \int_0^{\infty} \frac{[\epsilon_r'(\theta) - \epsilon_r'(\omega)]}{\theta^2 - \omega^2} d\theta \ . \tag{D.9}$$

The following summarizes some of the features of the Kramers-Kronig relations:

- The Hilbert transform relates real and imaginary components of a causal function.

- Direct solution requires complete data over full spectrum for one component.
- Equation (D.8) can be thought of as an integral equation for the unknown component when there are some data for the other component.

Another form of the dispersion relations is

$$\epsilon'_r(\omega) - \epsilon'(\omega_o) = -\frac{\omega - \omega_o}{\pi} P \int_{-\infty}^{\infty} \frac{\epsilon''_r(\theta) d\theta}{(\theta - \omega)(\theta - \omega_o)} , \tag{D.10}$$

$$\epsilon''_r(\omega) - \epsilon''(\omega_o) = \frac{\omega - \omega_o}{\pi} P \int_{-\infty}^{\infty} \frac{\epsilon'_r(\theta) d\theta}{(\theta - \omega)(\theta - \omega_o)} , \tag{D.11}$$

where P denotes principal value.

*U.S. GOVERNMENT PRINTING OFFICE:1994-573-013/89064